Nonlinear Subband Spline Adaptive Filter

Chang Liu, Xueliang Liu , Zhi Zhang and Xiao Tang
School of Electronic Engineering, Dongguan University of Technology, No.1 DaXueRoad, Dongguan, China
chaneaaa@163.com, liuxueliang83@163.com ,{zhangz, tangx}@dgut.edu.cn

Keywords: Subband adaptive filter, Nonlinear spline adaptive filter, adaptive filter algorithm, system identification.

Abstract: It has been reported that a novel class of nonlinear spline adaptive filter (SAF) obtains some advantages in modeling the nonlinear systems. In this paper, a nonlinear subband structure based on the spline adaptive filters, called subband spline adaptive filter (SSAF) is presented. The proposed structure is composed of a series of subband spline filters, each one comprises a linear time invariant (LTI) filter followed by an adaptive look-up table (ALUT). In addition, the computational complexity is also analyzed. Some experimental results in the context of the nonlinear system identification demonstrate the robustness of the proposed structure.

1 INTRODUCTION

In many practical engineering applications, the nonlinear system identification is an important and difficult task. Much well-established theory for linear system identification is unavailable when it comes to nonlinear case, so techniques to model the nonlinear behavior have been received more attention in recent decades (Mathews, 2000). In order to model the nonlinearity, several adaptive nonlinear structures have been introduced. Truncated Volterra adaptive filter (VAF) (Schetzen, 1980) is one of the most popular nonlinear model. However, its computational complexity be-comes huge with the increase of the nonlinear order. Neural Networks (NNs) (Haykin, 2009) can make a good des-cription of the nonlinear relation between the input signal and the current output adequately, but it suffers from a large computational cost and diffi-culties in on-line adaptation. Block-oriented archi-tecture (Giri, 2010), including the Wiener model, Hammers-tein model and cascade model, originates from the different combination of the linear time invariant (LTI) filters and memoryless nonlinear functions. Recently, Scarpiniti et al. has proposed a novel class of nonlinear spline adaptive filter (SAF) structure, which also contains the Wiener spline filter (Scarpiniti, 2013), the Hammerstein spline filter (Scarpiniti, 2014) and the cascade spline filter (Scarpiniti, 2015). In this kind of structure, the nonlinearity is modelled by a spline function which can be repress-ented by the adaptive look-up table (ALUT), and the linear time invariant (LTI) filter is used for determining the memory effect. Both the control points belonging to ALUT and the coefficients of the LTI are adapted by using the sophisticated adaptive algorithms such as the least mean square (LMS) algorithm, normalized least mean square (NLMS) algorithm and affine projection algorithm (APA).

In this paper, extending the subband idea into the spline adaptive filter (SAF), a nonlinear subband spline structure, called subband spline adaptive filter (SSAF) is proposed. Each subband spline filter is composed of a LTI filter followed by an ALUT. Then main advantage of the proposed subband model is its improved convergence performance because of the decorrelating properties with no significant computational increasement.

2 SPLINE ADAPTIVE FILTER

The block diagram of a SAF is shown in Fig.1, which consists of an adaptive finite impulse response (FIR) filter followed by a nonlinear network. In the nonlinear network, the spline interpolater, connected behind the adaptive LUT, determines the number and the spacing of control points (knots) contained in the LUT.

The input of the SAF at time n is $x(n)$, $s(n)$ represents the output of the linear networks which is given by

Liu, C., Liu, X., Zhang, Z. and Tang, X.
Nonlinear Subband Spline Adaptive Filter.
In *3rd International Conference on Electromechanical Control Technology and Transportation (ICECTT 2018)*, pages 163-167
ISBN: 978-989-758-312-4

$$s(n) = \mathbf{w}^T(n)\mathbf{x}(n), \tag{1}$$

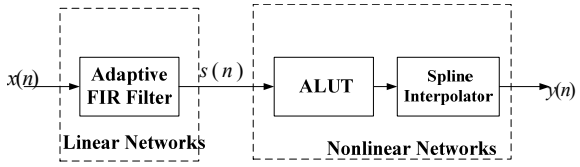

Figure 1: Block diagram of SAF.

where $\mathbf{w}(n) = [w_0, w_1, \cdots, w_{B-1}]^T$ represents the weight vector of the FIR filter with length B, and $\mathbf{x}(n) = [s(n), s(n-1), \cdots, s(n-B+1)]^T$ is the input vector of the linear network.

With reference to the spline interpolation scheme (Guarnieri, 1999), the output of the whole system $y(n)$ and $s(n)$ can be related by a local polynomial function $\varphi_i(u_n)$, which depends on the span index i and the local parameter u. The two parameters are defined as follows

$$u_n = s(n)/\Delta x - \lfloor s(n)/\Delta x \rfloor, \tag{2}$$

$$i_n = \lfloor s(n)/\Delta x \rfloor + (Q-1)/2, \tag{3}$$

where Δx is the uniform space between two control points for the function $\varphi_i(u_n)$, Q is the total number of control point and $\lfloor \cdot \rfloor$ denotes the floor operator. The output of the whole system can be expressed as

$$y(n) = \boldsymbol{\varphi}_i(u_n) = \mathbf{u}_n^T \mathbf{C} \mathbf{q}_{i,n}, \tag{4}$$

where $\mathbf{C}$ is the 4×4 spline basis matrix if the three-order spline function is used. Two suitable types of spline basis are B-spline and Catmull-Rom (CR) spline (Scarpiniti, 2013) which are given by

$$C_B = \frac{1}{6}\begin{bmatrix} -1 & 3 & -3 & 1 \\ 3 & -6 & 3 & 0 \\ -3 & 0 & 3 & 0 \\ 1 & 4 & 1 & 0 \end{bmatrix}, \; C_{CR} = \frac{1}{2}\begin{bmatrix} -1 & 3 & -3 & 1 \\ 2 & -5 & 4 & -1 \\ -1 & 0 & 1 & 0 \\ 0 & 2 & 0 & 0 \end{bmatrix}, \tag{5}$$

where $\mathbf{u}_n = [u_n^3, u_n^2, u_n, 1]^T$, $\mathbf{q}_{i,n} = [q_i, q_{i+1}, q_{i+2}, q_{i+3}]^T$ is the control point vector and superscript $(\cdot)^T$ denotes transposition.

3 SUBBAND SPLINE ADAPTIVE FILTER (SSAF)

Fig.2 shows the block diagram of the proposed SSAF. $\boldsymbol{\Phi}_0(\square)$ denotes the unknown nonlinear system which generates the desired signal $d(n) = \boldsymbol{\Phi}_0[x(n)]$ $v(n)$, where $x(n)$ is the system input. $v(n)$ is the background noise, assumed to be zero mean ,and independent of $x(n)$, its variance is σ_v^2. The input signal $x(n)$ and desired signal $d(n)$ are partitioned into M subband signals $x_m(n)$ and $d_m(n)$ via the analysis filters $H_m(z)$, $m = 0,1,\cdots,M-1$. The subband signals, $d_m(n)$ and $x_m(n)$ are critically decimated to a lower sampling rate commensurate with their bandwidth. We use the variable n to index the original sequences, and k to index the decimated sequence for all subband signals. The decimated output for the mth subband filter can be computed as

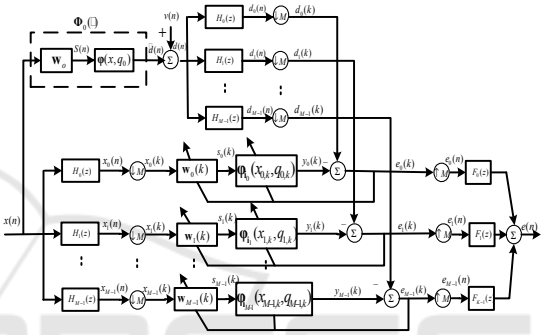

Figure 2: Block diagram of SSAF.

$$y_m(k) = \boldsymbol{\varphi}_{i_m}(u_{m,k}) = \mathbf{u}_{m,k}^T \mathbf{C} \mathbf{q}_{i_m,k}, \tag{6}$$

where $\mathbf{u}_{m,k} = [u_{m,k}^3, u_{m,k}^2, u_{m,k}, 1]^T$, $\mathbf{q}_{i_m,k} = [q_{i_m}, q_{(i+1)_m}, q_{(i+2)_m}, q_{(i+3)_m}]^T$ represents the mth subband control point vector at the decimated time k. The corresponding subband local parameter and subband span index i_m are defined as

$$u_{m,k} = s_m(k)/\Delta x_m - \lfloor s_m(k)/\Delta x_m \rfloor, \tag{7}$$

$$i_m = \lfloor s_m(k)/\Delta x_m \rfloor + (Q_m - 1)/2, \tag{8}$$

where Q_m is the total number of the control points for the mth subband LUT and Δx_m is the uniform space, which can be selected to different values for $m = 0,1,\cdots,M-1$. $s_m(k)$ is the output of the mth subband linear combiner which is given by

$$s_m(k) = \mathbf{w}_m^T(k)\mathbf{x}_m(k), \tag{9}$$

where $\mathbf{w}_m(k) = [w_{m,0}(k), w_{m,1}(k), \cdots, w_{m,B-1}(k)]^T$ denotes the weight vector of the subband FIR filter with length B. $\mathbf{s}_m(k) = [s_m(k), s_m(k-1), \cdots, s_m(k-B+1)]^T$ is the subband input vector.

The subband output error can be expressed as

$$e_m(k) = d_m(k) - y_m(k) \\ = d_m(k) - \boldsymbol{\varphi}_{i_m}(u_{m,k}), \quad (10)$$

It is realized that the adaptation in each subband is carried out independently as shown in Fig.2. Therefore, the updating equations of the linear and nonlinear networks for each subband can be derived by minimizing the cost function $\theta_m\left(\mathbf{w}_{m,k}, \mathbf{q}_{i_m,k}\right) = E\left\{\left|e_m(k)\right|^2\right\}$, where $E\{\cdot\}$ is the expectation operator. For analytical simplicity, using the instantaneous error instead of the expectation, we get

$$\theta_m\left(\mathbf{w}_{m,k}, \mathbf{q}_{i_m,k}\right) = e_m^2(k) \quad m = 0, 1, \cdots, M-1, \quad (11)$$

and taking the partial derivative $\theta_m\left(\mathbf{w}_{m,k}, \mathbf{q}_{i_m,k}\right)$ with respect to $\mathbf{w}_{m,k}$, we have

$$\frac{\partial \theta_m\left(\mathbf{w}_{m,k}, \mathbf{q}_{i_m,k}\right)}{\partial \mathbf{w}_{m,k}} = -2e_m(k) \frac{\partial \boldsymbol{\varphi}_{i_m}(u_{m,k})}{\partial u_{m,k}} \frac{\partial u_{m,k}}{\partial s_m(k)} \frac{\partial s_m(k)}{\partial \mathbf{w}^T(k)} \\ = -\frac{2}{\Delta x_m} e_m(k) \boldsymbol{\varphi}'_{i_m}(u_{m,k}) \mathbf{x}_m(k), \quad (12)$$

where $\boldsymbol{\varphi}'_{i_m}(u_{m,k})$ is the partial derivative of the local activation function for the mth subband, $\boldsymbol{\varphi}'_{i_m}(u_{m,k}) = \dot{\mathbf{u}}_{m,k}^T \mathbf{C} \mathbf{q}_{i_m,k}$, $\dot{\mathbf{u}}_{m,k} = [3u_{m,k}^2, 2u_{m,k}^1, 1, 0]^T$, so the updating equation of the linear networks for each subband can be given as

$$\mathbf{w}_m(k+1) = \mathbf{w}_m(k) + \frac{\mu_w}{\Delta x_m} e_m(k) \dot{\mathbf{u}}_{m,k}^T \mathbf{C} \mathbf{q}_{i_m,k} \mathbf{x}_m(k), \quad (13)$$

where μ_w is the step-size for the linear network adaptation.

For the subband nonlinear networks, the derivative calculation of $\theta_m\left(\mathbf{w}_{m,k}, \mathbf{q}_{i_m,k}\right)$ to $\mathbf{q}_{i_m,k}$ can be defined by

$$\frac{\partial \theta_m\left(\mathbf{w}_{m,k}, \mathbf{q}_{i_m,k}\right)}{\partial \mathbf{q}_{i_m,k}} = -2e_m(k) \frac{\partial \boldsymbol{\varphi}_{i_m}(u_{m,k})}{\partial \mathbf{q}_{i_m,k}} = -2e_m(k) \mathbf{C}^T \mathbf{u}_{m,k}, \quad (14)$$

The updating equation of the nonlinear networks for each subband can be written as

$$\mathbf{q}_{i_m,k+1} = \mathbf{q}_{i_m,k} + \mu_q e_m(k) \mathbf{C}^T \mathbf{u}_{m,k}, \quad (15)$$

4 COMPUTATIONAL COMPLEXITY

Note that (13) and (15) are the updating equations of the LMS algorithm for the proposed SSAF. For each iteration, only four control points for each subband are changed because of the local behavior of the spline function. This leads to a large computational savings. The computational complexity of the proposed SSAF solution is mainly evaluated in terms of the number of multiplications per sample. Note that for each subband , the control points of the LUT and the weights of the FIR filter are updated every M samples due to the critical sampling. Considering that there are M subband signals par-ticipating in the adaptation, it requires $2B+1$ multi-plications for the linear updating equation (13) and B multiplications for the output estimation of the linear network. For the spline output calculation and adap-tation, like the conventional SAF (Scarpiniti, 2013), we take into account of the repetitive appearance of the terms $\mathbf{C}\mathbf{q}_{i_m,k}$, $\mathbf{C}^T\mathbf{u}_{m,k}$ in (6), (13) and (15), it only needs $4K_q$ multiplications by the date reuse of the past computations, where K_q (less than 16) is the constant which can be defined with reference to the implementation spline structure in (Guarnieri, 1999). In addition, the subband input signal and desired signal partition needs $2MP$ multiplications, where P is the length of the analysis and synthesis filters. For error signal synthesis, it needs MP multiplications. Therefore, compared with the SAF scheme, the proposed one only requires extra $3MP$ multiplications for the subband signal analysis and synthesis.

5 EXPERIMENTAL RESULTS

To confirm the performance of the proposed scheme in this paper, we present the experimental results of the proposed scheme for the nonlinear system identification. All the following results are obtained by averaging over 50 Monte Carlo trials. The performance is measured by use of mean square error (MSE) defined as $10\log_{10}[e(n)]^2$. The input signal is generated by the process

$$x(n) = \omega x(n-1) + \sqrt{1-\omega^2}\,\beta(n), \quad (16)$$

where $\beta(n)$ is the White Gaussian noise signal with zero mean and unitary variance, the parameter ω is selected in the range $[0, 0.95]$, which interprets the degree of correlation for the adjacent samples. The FIR filter coefficients for the SAF and SSAF model

are initialized as $\mathbf{w}_{-1}=[\alpha,0,...,0]$ with length B and $0<\alpha\leq 1$, while the spline model is initially set to a straight line with a unitary slope. For convenience, only B-spline basis is applied in the simulations, however, the similar results can also be achieved using the CR-spline basis.

5.1 Experimental 1

The unknown system model $\mathbf{\Phi}_0(\cdot)$ is the Wiener spline model which comprises a FIR filter $\mathbf{w}_o=[0.6,-0.4,0.25,-0.15,0.1]^T$ and a nonlinear spline function represented by a 23 control points length LUT $\mathbf{q}_0$, Δx and Δx_m are set to 0.2 and $\mathbf{q}_0$ is defined by

$$\mathbf{q}_0=[-2.2,-2.0,-1.8,-1.6,-1.4,-1.2,-1.0,-0.8,-0.91,\\ -0.4,-0.2,0.05,0,-0.4,0.58,1.0,1.0,1.2,1.4,1.6,1,8,2.0,2.2], \tag{17}$$

For signal partitioning in this experiment, The cosine-modulated filter banks with subband number $K=2,4,$ and 8 are used and the prototype filters' length of analysis filter increases with the number of subband, the prototype filters' length , P, are 32 , 64 and 128 for $M=2,4,$ and 8 correspondently. The default values $\omega=0.5$, $\alpha=0.1$, and $B=5$ are employed and 10000 samples are used. An independent White Gaussian noise signal, $v(n)$, is added to the output of the unknown system, with 23-dB, 26-dB, 30dB signal to noise ratio (SNR) for $M=2,4,8$ respectively. The step sizes are selected to ensure that the conventional SAF and the SSAF obtain the similar steady-state MSE. The performances of the SAF and proposed SSAF are compared for the different numbers of subband in Fig.3. It can be seen that the proposed SSAF supplies the faster convergence rate than the SAF. This is due to the decorrelating properties of the subband scheme for colored input signals.

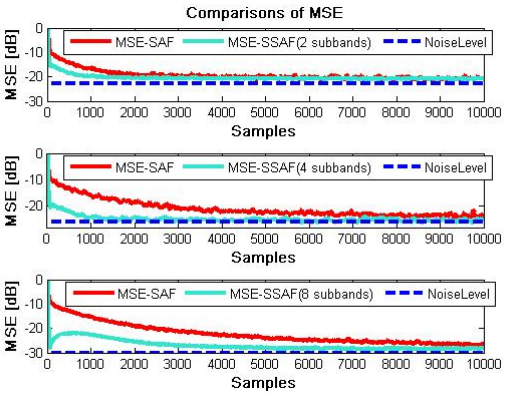

Figure 3: MSE curves of the SAF and SSAF.

5.2 Experimental 2

In the second experiment, we compare the MSE performance of the polynomial model (Stenger, 2000), 2-rd order Volterra model (Kuech, 2002), 2-rd order subband Volterra model (Burton, 2009), SAF model (Scarpiniti, 2013) and proposed SSAF model. The unknown system to be identified $\mathbf{\Phi}_0(\cdot)$ consists of two blocks, the first one is the 3-order IIR filter

$$H(z)=\frac{0.0154+0.046z^{-1}+0.0462z^{-2}+0.0154z^{-3}}{1-1.99z^{-1}+1.572z^{-2}-0.4583z^{-3}}, \tag{18}$$

and the second block nonlinearity

$$y(n)=\sin(x[n]). \tag{19}$$

The number of subband is set to 4 for the SSAF and 2-rd order subband Volterra model. The cosine-modulated filter banks with subband number $M=4$ are used and the prototype filters' length is selected to 64. The step sizes are set to $\mu_q=\mu_w=0.01$ for both the HSAF and the SSAF, step size $\mu=0.001$ is used for the polynomial model and the step size is set to 0.01 for the 2-rd order Volterra and 2-rd order subband Volterra model. The signal to noise ratio is $SNR=30dB$. The default values $\omega=0.6$, $\alpha=0.1$, $\Delta x=\Delta x_m=0.2$ and $B=15$ are employed and 50000 samples are used. A comparison of the MSE learning curves is reported in Fig. 4, it can be clearly noted that the robustness of the proposed SSAF.

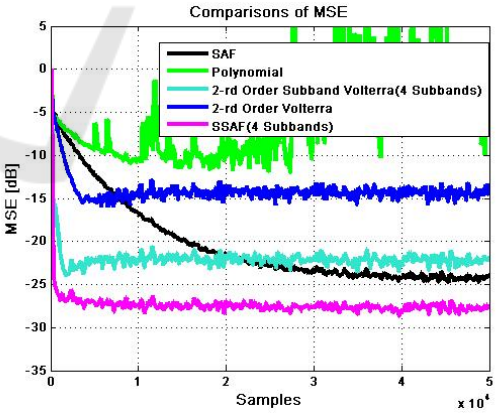

Figure 4: Comparison MSE of the different models in experiment 2.

5.3 Experimental 3

The third experiment aims to test the effectiveness of the proposed structure in case of a high degree of nonlinearity. The unknown system in system identification $\Phi_0(\cdot)$ comprises three blocks. The first and the last blocks are IIR filters whose transfer function can be written as

$$H_1(z)=\left(\frac{0.2851+0.5704z^{-1}+0.2851z^{-2}}{1-0.1024z^{-1}+0.4475z^{-2}}\right) \times\left(\frac{0.2025+0.2880z^{-1}+0.2025z^{-2}}{1-0.6591z^{-1}+0.1498z^{-2}}\right), \quad (20)$$

$$H_3(z)=\left(\frac{0.2025+0.2880z^{-1}+0.2025z^{-2}}{1-1.01z^{-1}+0.5861z^{-2}}\right) \times\left(\frac{0.2025+0.2880z^{-1}+0.2025z^{-2}}{1-0.6591z^{-1}+0.1498z^{-2}}\right), \quad (21)$$

and the nonlinear portion of this model is expressed by

$$y(n)=\frac{2x(n)}{1+|x(n)|^2}. \quad (22)$$

It is noted that this model is capable of describing the behavior model of the radio frequency amplifier for satellite communications (Scarpiniti, 2013). For both the SAF and the SSAF, linear filter length B is set to 15. The parameter ω is set to 0.2. All the other parameters are set to similar values as in Experimental 2. Fig. 5 shows that the comparison of the MSE learning curves for several models, it is clear in this case that the deteriorating performance of the Polynomial model and the 2-rd order Volterra model, verifying that these two models only cope with the case of mile nonlinearity. Furthermore, the proposed SSAF obtains the best convergence performance with respect to other models.

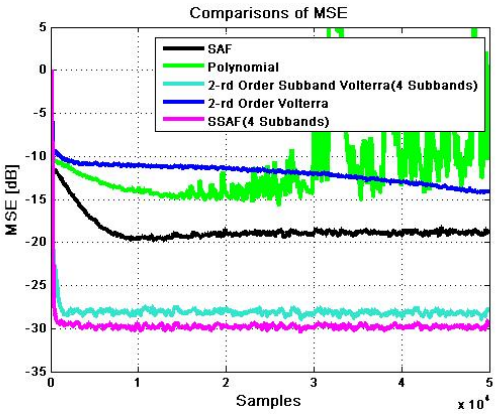

Figure 5: Comparison MSE of the different models in experiment 3.

6 CONCLUSIONS

In this paper, a novel SSAF structure for nonlinear system identification is presented. It consists of a series of subband nonlinear filters, the adaptation of these subband filters is carried out independently. The computational complexity is analyzed based on the LMS algorithm. Some experimental results in the context of the nonlinear system identification show the effectiveness of the proposed structure.

ACKNOWLEDGEMENTS

This research was supported by the National Natural Science Foundation of China (61501119).

REFERENCES

Mathews V.J., Sicuranza G.L., 2000. *Polynomial Signal Processing.* John Wiley & Sons, Hoboken, New Jersey.

Schetzen M., 1980. *The Volterra and Wiener Theories of Nonlinear Systems*, John Wiley & Sons, New York,.

Haykin S., 2009. *Neural Networks and Learning Machines*, Pearson Publishing, 2nd ed.

Giri F., Bai E.W., (Eds.), 2010. *Block-Oriented Nonlinear System Identification,* Springer-Verlag, Berlin.

Scarpiniti M., Conniniello D., Parisi R., Uncini A., 2013. *Nonlinear spline adaptive filtering*, Signal Proce-ssing 93(4) 772–783.

Scarpiniti M., Conniniello D., Parisi R., Uncini A., 2014. *Hammerstein uniform cubic spline adaptive filtering: Learning and convergence properties*, Si-gnal Processing 100(4) 112–123.

Scarpiniti M., Conniniello D., Parisi R., Uncini A., 2015. *Novel cascade spline architectures for the identification of nonlinear systems*, IEEE Tran-sanctions on Circuits and Systems-I: regular papares 62(7) 1825-1835.

Guarnieri S., Piazza F., Uncini A., 1999. *Multilayer feedforward networks with adaptive spline activation function*, IEEE Transanctions on Neural Networks, 10(3) 672-683.

Burton T. G., Goubran R.A., 2009. Beaucoup F., *Nonlinear system identification using a sub-band adaptive Volterra filter*, IEEE Transanctions on Instrumentation and Measurement, 58(5) 1389-1397.

Stenger S., Kellerman W., 2000. *Adaptation of a memoryless preprocessor for nonlinear acoustic echo cancelling*, Signal Processing, 80(9) 1747–1760.

Kuech F., Kellerman W., 2002. *Nonlinear line echo cancellation using a simplified second order Volterra filter*, in *Proceedings of the ICASSP,* vol. 2, Orlando, Flo-rida, 1117–1120.